Kit^{cre} knock-in mice fail to fate-map cardiac stem cells

ARISING FROM J. H. van Berlo *et al. Nature* **509,** 337–341 (2014); doi:10.1038/nature13309

In a cell fate-mapping study[1] using a *cre*-knock-in (KI) into the *Kit* locus, and in two other studies that used a similar genetic approach to track the fate of cardiac stem/progenitor cells (CSCs)[2,3], the authors concluded that c-Kit^{pos} (also known as Kit^{pos}) cells only negligibly contributed to the generation of cardiomyocytes. These studies questioned our findings[4] that tissue-specific c-Kit^{pos} CSCs are endogenous regenerative agents that are necessary and sufficient for cardiomyocyte regeneration/replenishment after injury. There is a Reply to this Comment by van Berlo, J. H. *et al. Nature* **555,** http://doi.org/10.1038/nature25772 (2018).

For these differences to be resolved, it is necessary to confirm that the *Kit*^{cre}-KI approach[1] correctly identifies and fate-maps c-Kit^{pos} CSCs and/or investigate whether the insertion of *Kit*^{cre}-KI affects CSC biology and cardiomyogenic potential.

We used tamoxifen-inducible *Kit*$^{CreER(T2)/+(5-7)}$, *Kit*$^{MerCreMer/+}$ (hereafter *Kit*$^{MCM/+}$)[1,2] and constitutive *Kit*$^{CreGFPnls/+}$ (ref. 1) mouse lines, which are phenotypically similar to *Kit*$^{W/+}$ mice[5]. These mice have white spotting in their fur coat, a 50% decrease in c-Kit expression (Extended Data Fig. 1a) and a testis growth deficit (with low fertility) when heterozygous, this genotype shows fetal/postnatal lethality in homozygotes[1–3,6–8].

The efficiency of recombination by the Cre–*loxP* system is proportional to the level of Cre expression and the duration of Cre expression in each cell[9–11], which in these *Kit*^{cre}-KI lines depends on the endogenous *Kit* promoter. In mice, different c-Kit^{pos} cell types express different levels of c-Kit, with mast cells being the highest c-Kit-expressing cells[5–7]. In the adult mouse heart, the majority of c-Kit^{pos} cells ($\geq$90%) are committed to the blood cell lineage, expressing markers such as CD45 and CD31 (and are lineage positive (Lin^{pos})) (Fig. 1a). Only a minority ($<$10%) of c-Kit^{pos} cardiac cells are CD45^{neg}CD31^{neg} (Lin^{neg}) (Fig. 1a). These Lin^{neg}c-Kit^{pos} cardiac cells are enriched for and include all of the adult CSCs, which comprise only approximately 10% of these cells[12,13]. This subset expresses low but clearly detectable levels of *Kit* mRNA and c-Kit protein (Extended Data Fig. 1b), which are significantly lower than the levels found in Lin^{pos}c-Kit^{pos} cardiac cells (Extended Data Fig. 1b). Single wild-type Lin^{neg}c-Kit^{pos} clonogenic and multipotent CSCs show significantly lower *Kit* expression, at the mRNA and protein levels, than embryonic stem cells, haematopoietic stem cells (HSCs) and bone marrow mast cells (Extended Data Fig. 1c, d). Accordingly, Cre$^{ER(T2)}$ protein and mRNA expression in bone marrow mast cells is robust, whereas it is only faintly detectable in freshly isolated Lin^{neg} CSCs (Extended Data Fig. 1e, f). This heterogeneity in cell types that have different levels of c-Kit expression, the low abundance of CSCs among the c-Kit^{pos} cardiac cells and the very low levels of c-Kit expression in CSCs highlight the difficulties of using *Kit*^{cre}-KI to track the fate of the CSCs.

Kit$^{CreER(T2)/+}$ mice[6–8] were crossed with homozygous global double-fluorescent Cre-reporter *Rosa26*$^{mT/mG}$ mice[14] (Extended Data Fig. 2a), expressing a membrane-targeted tandem Tomato dimer (mT) that switches to a membrane-targeted GFP (mG) after Cre-dependent recombination[14].

When double-mutant *Kit*$^{CreER(T2)/+}$:*Rosa26*$^{mT/mG/+}$ mice were given a standard tamoxifen diet for 14 days, 80 $\pm$ 8% of the c-Kit^{pos} bone marrow mast cells showed Cre-dependent recombination and expressed GFP, whereas less than 5% of HSCs showed recombination and GFP expression (Extended Data Fig. 1g–j). At the same time, $\leq$20% of all c-Kit^{pos} cardiac cells were recombined (Extended Data Fig. 1k), but all of these were CD45^{pos}, CD31^{pos} or both, representing cardiac mast cells or endothelial progenitor cells (Extended Data Fig. 1l). By contrast, the CSC-enriched Lin^{neg}c-Kit^{low} cells showed minimal recombination ($\leq$1%) and expression of GFP (Extended Data Fig. 1l). Using the *Kit*$^{MCM/+}$:*Rosa26*$^{mT/mG/+}$ mice from van Berlo *et al.*[1] yielded almost identical results (Extended Data Fig. 3a–c).

To increase the probability of recombination by extending the duration of Cre expression, 8-week-old double-mutant *Kit*$^{CreER(T2)/+}$:*Rosa26*$^{mT/mG/+}$ mice received a tamoxifen diet for four months[1] (Fig. 1b–e). This regime showed efficient recombination in several tissue-specific c-Kit-expressing cells (Extended Data Fig. 2b). In the bone marrow, approximately 80% of the total number of cells and up to 60% of c-Kit^{pos} cells became GFP^{pos} (Extended Data Fig. 2c). Analysis of bone marrow cell sub-populations showed that approximately 100% of c-Kit^{pos} mast cells were GFP^{pos} (Extended Data Fig. 2d), whereas only $\leq$35% of HSCs expressed GFP (Extended Data Fig. 2e). As expected, recombination events were increased further by constitutive *Kit*^{cre} expression in *Kit*$^{CreGFPnls/+}$:*Rosa26*$^{mT/mG/+}$ double-heterozygous mice (Extended Data Fig. 2g–j).

Fluorescence-activated cell sorting (FACS) of dissociated total cardiac cells showed that around 15% of cells showed Cre-mediated recombination and GFP expression (Fig. 1b). Among the total c-Kit antibody-labelled cells, 65 $\pm$ 5% were GFP^{pos} (Fig. 1c). Immunohistochemistry of frozen cardiac sections confirmed that approximately 60% of c-Kit antibody-labelled cells had turned GFP^{pos} (Extended Data Fig. 2f). The majority of these GFP^{pos} cells were still mT^{pos} (Fig. 1b, c), highlighting its slow decay in myocardial tissue[14]. Nevertheless, 80% of the endothelial/mast cell lineage-committed Lin^{pos}c-Kit^{pos} cells were GFP^{pos}, whereas only $\leq$10% of the CSC-enriched Lin^{neg}c-Kit^{low} cardiac cells showed recombination (Fig. 1d). Experiments using *Kit*$^{MCM/+}$ mice[1] yielded similar findings (data not shown).

After mice were fed the tamoxifen diet for four months, only 0.04 $\pm$ 0.01% cardiomyocytes were GFP^{pos}, and most of those cells were also mT^{pos} (Fig. 1e). van Berlo *et al.*[1] interpreted the presence of double-labelled mT^{pos} and GFP^{pos} cardiomyocytes as the evidence of fusion between a pre-existing *Rosa26*$^{mT/mG/+}$ cardiomyocyte and a *Kit*$^{cre/+}$cell. However, because myocardial decay of mT is very slow[14], mT/mG double-positive cardiomyocytes are most likely the consequence of the very slow decay of mT in randomly and progressively recombined progenitors that differentiate into cardiomyocytes.

Similar results were obtained when using 8–12-week-old *Kit*$^{CreGFPnls/+}$:*Rosa26*$^{mT/mG/+}$ double-heterozygous mice (Fig. 1f–i) and *Kit*$^{CreGFPnls/+}$ mice crossed with *Rosa26*$^{floxed\text{-}stop\text{-}tdTomato}$ mice (Extended Data Fig. 3d–f).

We sorted and cultured Lin^{neg}c-Kit^{pos} CSCs from *Kit*$^{CreER(T2)/+}$:*Rosa26*$^{mT/mG/+}$ double-heterozygous mice in the presence or absence of tamoxifen *in vitro*. Tamoxifen induced recombination in $\leq$1% of the Lin^{neg}c-Kit^{pos} cells and expression of GFP (Fig. 1j), whereas $>$95% of bone-marrow-derived mast cells showed recombination within seven days (Fig. 1k). None of the single-cell-derived CSC clones that were generated in medium with tamoxifen at passage (P)4

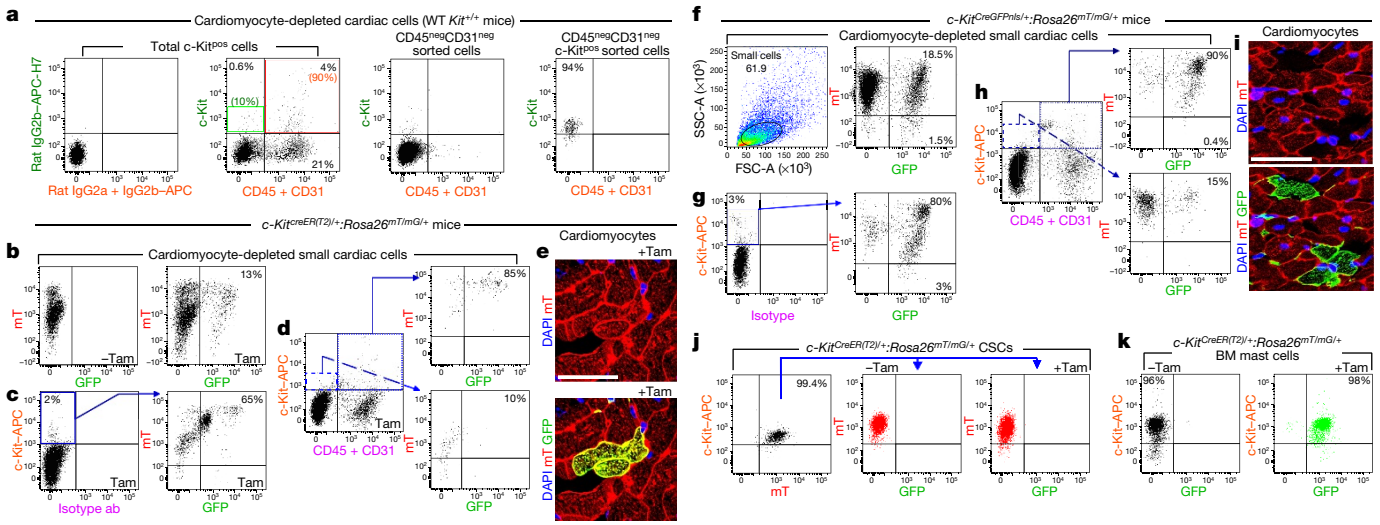

Figure 1 | *Kit*^{cre} genetic lineage cell tracking tags only a minimal fraction of CSCs *in vivo* and *in vitro*. **a**, Left, flow cytometry dot plots show that the majority of c-Kit^{pos} cardiac cells are also CD45^{pos} or CD31^{pos} (red box), whereas only a minority are CD45^{neg} and CD31^{neg} (green box). Right, flow cytometry plots show that CD45^{pos}CD31^{pos}(Lin^{pos}) cells are efficiently removed from cardiac cells by negative sorting and CD45^{neg}CD31^{neg}c-Kit^{pos}-sorted cells uniformly express low levels of c-Kit. The panels show an experiment with sequential analysis of unsorted cells (left) and re-analysis of sorted cells (right) from cardiomyocyte-depleted cells obtained from five enzyme-digested and pooled hearts. Representative of $n = 3$ experiments. **b**, Representative FACS plots showing that the tamoxifen (Tam) diet for four months induces GFP expression in 15% of all cardiac cells from *Kit*$^{CreER(T2)/+}$:*Rosa26*$^{mT/mG/+}$ mice. No GFP signal is detected if the mice were not fed the tamoxifen diet. **c**, Approximately 70% of c-Kit-labelled cardiac cells were GFP^{pos} after the mice were fed the tamoxifen diet. Almost all of these GFP^{pos} cells were still mT^{pos}. **d**, The majority of c-Kit^{pos} cardiac cells are CD45^{pos} (labelled with CD45–PE-Vio) or CD31^{pos} (labelled with CD31–PE-Vio) and around 80% of them are recombined to express GFP, whereas $\leq 10\%$ of the CSC-enriched CD45^{neg}CD31^{neg}c-Kit^{pos} cardiac cells became GFP^{pos}. Almost all of these GFP^{pos} cells were still mT^{pos}. **b**–**d**, Representative of $n = 5$ hearts. **e**, Confocal image showing recombined GFP^{pos} cardiomyocytes after four months of tamoxifen diet in *Kit*$^{CreER(T2)/+}$:*Rosa26*$^{mT/mG/+}$ mice. These cardiomyocytes still express mT. Representative of $n = 5$ hearts. Scale bar, 20 μm. **f**, Approximately 20% of all cardiac cells of 8–12-week-old *Kit*$^{CreGFPnls/+}$:*Rosa26*$^{mT/mG/+}$ mice are GFP^{pos}. **g**, Approximately 80% of c-Kit^{pos} cardiac cells are GFP^{pos} from same mice. **h**, Around 90% of endothelial/mast cell lineage-committed, CD45^{pos}CD31^{pos}c-Kit^{pos} cardiac cells are recombined to express GFP, whereas fewer than 20% of the CSC-enriched CD45^{neg}CD31^{neg}c-Kit^{pos} were recombined to become GFP^{pos}. **f**–**h**, Representative of $n = 5$ hearts. Note that GFP-expressing cells in **f**–**h** are mostly still mT^{pos}. **i**, Confocal image showing recombined GFP^{pos} cardiomyocytes (around 0.25% of all cardiomyocytes) in 8–12-week-old *Kit*$^{CreGFPnls/+}$:*Rosa26*$^{mT/mG/+}$ mice. Representative of $n = 5$ hearts. Scale bar, 20 μm. Most of these cardiomyocytes do not express mT. **j**, Representative flow cytometry plots showing that tamoxifen *in vitro* is unable to recombine c-Kit^{pos} CSCs isolated from *Kit*$^{CreER(T2)/+}$:*Rosa26*$^{mT/mG/+}$ mice. $n = 5$ biological replicates. **k**, Tamoxifen addition *in vitro* induced recombination in all bone-marrow (BM)-derived mast cells. $n = 5$ biological replicates.

were GFP^{pos}. Additionally, when Lin^{neg}c-Kit^{pos} cardiac cells from *Kit*$^{CreGFPnls/+}$:*Rosa26*$^{mT/mG/+}$ double-heterozygous mice were cloned, only 1 out of 19 CSC clones (from 1,056 deposited single cells, 116 of which were GFP^{pos}) was GFP^{pos}. When 10 randomly selected GFP^{neg} clones were expanded for up to 10 passages, only $8 \pm 3\%$ cells within each clone became GFP^{pos}.

Together, these data show that *Kit*^{cre} alleles, inducible and constitutive, in the cardiac Lin^{neg}c-Kit^{low} cell pool, which includes multipotent CSCs, recombine very inefficiently, stochastically and do not reliably track the fate of Lin^{neg}c-Kit^{low} CSCs.

Kit^{cre}-KI null alleles are phenotypically equivalent to severe W mutations that affect the molecular and phenotypic properties of c-Kit-expressing cells[5,15]. We therefore evaluated the growth, self-renewal and myogenicity of freshly isolated CSC-enriched Lin^{neg}c-Kit^{pos} cardiac cells and of single-cell-derived c-Kit^{pos} CSC clones obtained from *Kit*$^{CreER(T2)/+}$ mice (hereafter, W^{Cre} CSCs) compared to freshly isolated and cloned *Kit*$^{+/+}$ CSCs from wild-type littermates. Freshly isolated W^{Cre} CSCs at P1 showed a significant growth delay and lower BrdU incorporation in response to serum, and formed fewer single-cell-derived clones and cardiospheres compared to wild-type CSCs (Fig. 2a–c). Similar data were obtained with CSC-enriched Lin^{neg}c-Kit^{pos} cardiac cells from *Kit*$^{CreGFPnls/+}$ mice (Extended Data Fig. 4a). When tested for cardiomyogenic differentiation[12,13], wild-type CSC-derived cardiospheres homogenously differentiated into cardiac troponin I (cTnI)-expressing cells (Fig. 2d), exhibited vigorous spontaneous rhythmic contractions (Supplementary Video 1), and showed upregulation of the main cardiomyocyte-specific genes (Fig. 2e). By contrast, cardiospheres from W^{Cre} CSCs rarely differentiated into cTnI-positive cells and sparingly showed rare/weak beating (Fig. 2d). Accordingly, cardiac-specific gene transcripts were minimally upregulated (Fig. 2e). RNA-sequencing-based analysis of whole-cell transcriptomes of cloned W^{Cre} CSCs and wild-type CSCs confirmed that c-Kit heterozygosity affected the expression of genes associated with RNA transcription, cardiac development, and cell growth, survival and death (Extended Data Fig. 4b, c).

To test whether restoring normal levels of c-Kit expression would correct defects in the stemness potential of W^{Cre} CSCs *in vitro* and *in vivo*, we transfected a bacterial artificial chromosome (BAC) construct spanning the entire *Kit* gene locus into cloned mT-W^{Cre} CSCs (from *Kit*$^{CreER(T2)/+}$:*Rosa26*$^{mT/mG/+}$ mice). Using qPCR, we selected one clone with a single BAC^{Kit} copy (hereafter mT-BAC^{Kit}W^{Cre} CSCs) that expressed *Kit* mRNA and c-Kit protein at levels similar to those of mT wild-type (mT-WT) CSCs (from *Rosa26*$^{mT/mG/+}$ littermates) (Fig. 2f and Extended Data Fig. 4d, e). The defects in cell growth, clonogenesis, cardiosphere formation and myogenic differentiation of mT-W^{Cre} CSCs were completely rescued by BAC^{Kit} transfection. The mT-BAC^{Kit}W^{Cre} CSCs phenotype is indistinguishable from that of mT-WT CSCs (Fig. 2g, h and Extended Data Fig. 4f–h).

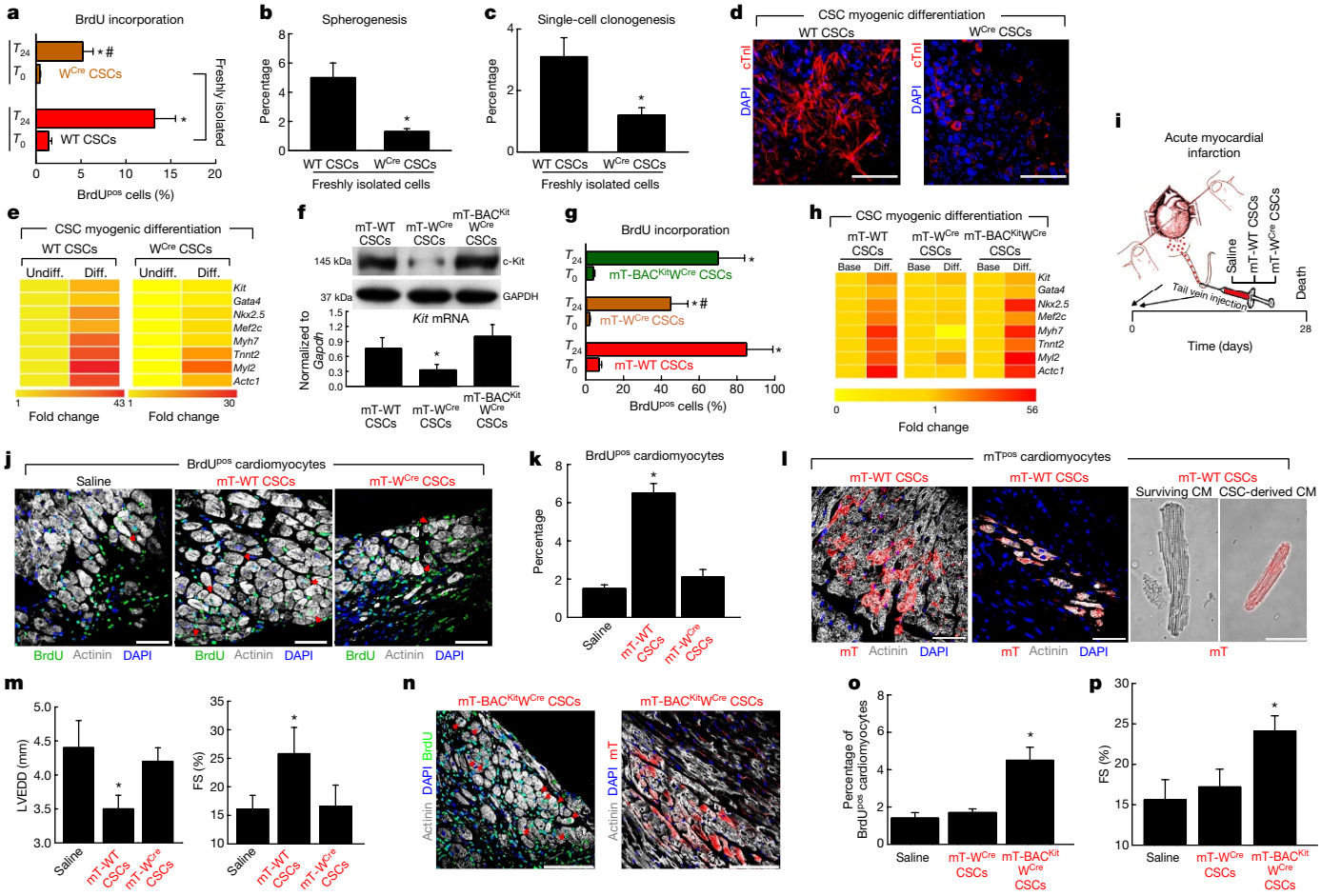

Figure 2 | The *W*^{cre} allele impairs c-Kit^{pos} adult CSC myogenic and regenerative properties. **a**, Serum-induced 24 h BrdU incorporation in freshly isolated W^{Cre} CSCs compared to wild-type (WT) CSCs. $*P < 0.05$ vs. T_0 (before addition); $\#P < 0.05$ compared to wild-type CSCs. **b**, W^{Cre} CSCs formed fewer cardiospheres than wild-type CSCs. 1×10^5 plated cells. **c**, Clonal efficiency of freshly isolated W^{Cre} CSCs versus wild-type CSCs. **b**, **c**, $*P < 0.05$ versus wild-type CSCs. **d**, cTnI expression in cardiospheres from cloned wild-type CSCs and W^{Cre} CSCs after 14 days in myogenic medium. Scale bar, 50 μm. **a**–**d**, Representative of $n = 5$ biological replicates. **e**, Heat map showing qPCR analysis of main cardiomyocyte genes in cardiospheres from cloned wild-type and W^{Cre} CSCs after 14 days in myogenic medium. $n = 3$ biological replicates. **f**, Normalization of *Kit* mRNA and protein expression in mT-BAC^{Kit}W^{Cre} CSCs compared to mT-WT CSCs and naive mT-W^{Cre} CSCs. $*P < 0.05$ compared to all other treatments. $n = 3$ biological replicates. **g**, BrdU incorporation in mT-BAC^{Kit}W^{Cre} CSCs compared to mT-W^{Cre} CSCs and mT-WT CSCs. $*P < 0.05$ versus T_0; $\#P < 0.05$ versus T_{24}. $n = 4$ biological replicates. **h**, Heat map of qPCR analysis of the modulation of main cardiomyocyte genes in cardiospheres from mT-BAC^{Kit}W^{Cre} CSCs compared to mT-W^{Cre} CSCs and mT-WT CSCs after 14 days in myogenic medium. Representative of $n = 3$ biological replicates. **i**, Myocardial infarction (MI) study design. **j**, BrdU incorporation (red arrows point at BrdU^{pos} cardiomyocytes) in the border zone of infarcted hearts from wild-type (WT) mice treated with either saline ($n = 6$) or with the indicated CSC types. Scale bar, 50 μm. **k**, Newly generated BrdU^{pos} cardiomyocytes 28 days after myocardial infarction in wild-type mice treated with either saline or with the indicated CSC types. $*P < 0.05$ versus all other treatments. **j**–**m**, $n = 6$ mice per group. **l**, Left, CSC-derived mT^{pos} cardiomyocytes in the border zone of infarcted hearts from mice treated with mT-WT CSCs. Note that, in the middle panel, mT^{pos} cardiomyocytes remuscularize proper infarct zone. Right, single cardiomyocytes dissociated from the hearts of additional three mice with a myocardial infarction. A living mT-fluorescing CSC-derived bona fide cardiomyocyte (CM) is shown opposite a host surviving cardiomyocyte. Scale bar, 50 μm. **m**, Left ventricular function 28 days after myocardial infarction in wild-type mice treated with either saline or with the indicated CSCs types. $*P < 0.05$ versus saline and mT-W^{Cre} CSCs. LVEDD, left ventricle end diastolic diameter; FS, fractional shortening. **j**, **k**, **m**, $n = 6$ mice per group. **n**, BrdU^{pos} cardiomyocytes (red arrows) in the border zone of infarcted hearts from wild-type mice treated with mT-BAC^{Kit}W^{Cre} CSCs. Scale bar, 50 μm. **o**, Percentage of newly generated BrdU^{pos} cardiomyocytes 28 days after myocardial infarction in wild-type mice treated with saline ($n = 6$), mT-W^{Cre} CSCs ($n = 6$) or mT-BAC^{Kit}W^{Cre} CSCs ($n = 6$). $*P < 0.05$ versus all other treatments. **p**, Echocardiography assessment of left ventricular function (fractional shortening) 28 days after myocardial infarction in wild-type mice treated with either saline or the indicated CSC types. $*P < 0.05$ versus all other treatments. *n* values as in **o**. All data are mean ± s.d.

To test the effect of the *Kit*^{cre}-KI mutations on cardiac repair/regeneration, *Kit*$^{CreGFPnls/+}$:*Rosa26*$^{mT/mG/+}$ double-heterozygous mice and *Rosa26*$^{mT/mG/+}$ heterozygous controls were subjected to myocardial infarction followed by systemic BrdU administration. At 28 days after myocardial infarction, *Kit*$^{CreGFPnls/+}$:*Rosa26*$^{mT/mG/+}$ mice had significantly larger infarcts and lower number of BrdU^{pos} cardiomyocytes in the infarct border zone than *Rosa26*$^{mT/mG/+}$ heterozygous controls (0.4 ± 0.14 compared to 1.1 ± 0.15%, respectively; $P < 0.05$) (Extended Data Fig. 5a–d). The number of c-Kit^{pos} cell-generated GFP^{pos} cardiomyocytes in *Kit*$^{CreGFPnls/+}$:*Rosa26*$^{mT/mG/+}$

mice after myocardial infarction was only slightly higher than in the sham-operated controls ($0.28 \pm 0.04\%$ compared to $0.4 \pm 0.2\%$, respectively; $P > 0.05$, not significant) (Extended Data Fig. 5e–g). The lower number of newly generated GFP^{pos} or BrdU^{pos} cardiomyocytes in *Kit*$^{CreGFPnls/+}$:*Rosa26*$^{mT/mG/+}$ compared to *Rosa26*$^{mT/mG/+}$ mice correlated inversely with increased hypertrophy of the residual cardiomyocytes (Extended Data Fig. 5h, i) and reduced arteriolar and capillary density (Extended Data Fig. 5j, k) in the infarct border zone. Concordantly, left ventricular dysfunction was more severe in *Kit*$^{CreGFPnls/+}$:*Rosa26*$^{mT/mG/+}$ than in *Rosa26*$^{mT/mG/+}$ mice (Extended Data Fig. 5l, n). These data demonstrate that the *W*^{cre} allele negatively affects the myogenicity of the CSCs, but cannot address whether the latter is the main mechanism that underlies the worsened cardiac remodelling after myocardial infarction in *Kit*^{cre} mice. This is because c-Kit haploinsufficiency could also affect additional repair/regeneration processes other than cardiomyocyte replacement.

We next transplanted 4×10^5 cloned W^{Cre} CSCs obtained from *Kit*$^{CreER(T2)/+}$:*Rosa26*$^{mT/mG/+}$ mice (hereafter mT-W^{Cre} CSCs) or the same number of wild-type CSCs from *Rosa26*$^{mT/mG/+}$ littermates (mT-WT CSCs) or saline into the systemic circulation 30 min after myocardial infarction in three groups of C57BL/6J mice (Fig. 2i). After 28 days, recipients of mT-WT CSCs had a significant higher number of BrdU^{pos} cardiomyocytes in the infarct border zone than the mT-W^{Cre} CSCs- and saline-injected mice ($6.5 \pm 0.5\%$ compared to $2.0 \pm 0.4\%$ and $1.5 \pm 0.2\%$, respectively; $P < 0.05$) (Fig. 2j, k). The mT-WT CSCs generated a significant number of mT^{pos} cardiomyocytes within the infarct border zone ($3.5 \pm 0.5\%$) with foci of re-muscularized tissue within the proper infarct zone (Fig. 2l). This result was confirmed by identifying abundant mature mT^{pos} cardiomyocytes in dissociated myocardial cells (Fig. 2l) together with a notable improvement in arteriole and capillary density in the mT-WT CSC-injected mice. By contrast, only very small numbers of mT^{pos} cardiomyocytes with scarce arterioles and capillaries were detected in the infarct border zone of the mT-W^{Cre} CSC-injected mice (Extended Data Fig. 6a-d). Not surprisingly, whereas mT-WT CSCs significantly improved left ventricular function over saline injection, mT-W^{Cre} CSCs did not (Fig. 2m).

In concordance with the results presented above, BAC^{Kit} transgenesis also completely rescued regenerative defects of the W^{Cre} CSCs (Fig. 2n–p and Extended Data Fig. 6e–g). The beneficial effects of mT-BAC^{Kit}W^{Cre} CSCs transplantation on myocardial remodelling and function after myocardial infarction (Fig. 2n–p and Extended Data Fig. 6e–g) were qualitatively and quantitatively similar to those produced by mT wild-type CSCs (see Fig. 2j–m and Extended Data Fig. 6a–d).

To directly test whether cell fusion, not CSC-derived neomyogenesis (see ref. 1), causes the appearance of double-labelled mT/mG cardiomyocytes after wild-type CSC transplantation, mT-WT CSCs from *Rosa26*$^{mT/mG}$ mice (mT^{pos}) were injected into *Tg*$^{Myh6\text{-}MCM}$ mice after myocardial infarction. Mice were then fed with the tamoxifen diet for 28 days. Invariably, all the mT^{pos} cardiomyocytes were only mT^{pos} and none expressed GFP (see Extended Data Fig. 6h–j).

These data show that harvested endogenous CSCs are robustly myogenic *in vitro* and *in vivo* and, while they do not further address whether and/or to what extent c-Kit^{pos} CSCs contribute to endogenous cardiac regeneration (but see ref. 4), they do reveal several limitations of the use of *Kit*^{cre}-KI strategies for CSC identification and cell-fate mapping. The very low number of endogenous c-Kit^{pos} CSC-generated cardiomyocytes detected in the *Kit*^{cre} mice simply reflects the failure to recombine the CSCs to track their progeny and the severe defect in CSC myogenesis produced by the *Kit*^{cre} allele.

This work was supported by grants from CARE-MI FP7 (Health-F5-2010-242038) large-scale collaborative project, M.I.U.R. FIRB-Futuro-in-Ricerca (RBFR12I3KA), M.I.U.R. PRIN2015 (2015ZTT5KB_004), and the Italian Ministry of Health (GR-2010-2318945).

Data Availability RNA-sequencing data are available in GEO with the accession number GSE102002.

Carla Vicinanza[1]*, Iolanda Aquila[1]*, Eleonora Cianflone[1], Mariangela Scalise[1], Fabiola Marino[1], Teresa Mancuso[1], Francesca Fumagalli[2], Emilia Dora Giovannone[3], Francesca Cristiano[4], Enrico Iaccino[1], Pina Marotta[1], Annalaura Torella[5], Roberto Latini[2], Valter Agosti[3], Pierangelo Veltri[4], Konrad Urbanek[6], Andrea M. Isidori[7], Dieter Saur[8,9], Ciro Indolfi[1], Bernardo Nadal-Ginard[1]§ & Daniele Torella[1]§

[1]Molecular and Cellular Cardiology, Department of Medical and Surgical Sciences, Magna Graecia University, Catanzaro 88100, Italy.
emails: bernardo.nadalginard@gmail.com; dtorella@unicz.it
[2]IRCCS - Istituto di Ricerche Farmacologiche "Mario Negri", Milan 20156, Italy.
[3]CIS for Genomics and Molecular Pathology, Magna Graecia University, Catanzaro 88100, Italy.
[4]Bioinformatics, Department of Medical and Surgical Sciences, Magna Graecia University, Catanzaro 88100, Italy.
[5]Department of Biochemistry, Biophysics and General Pathology, University of Campania "L. Vanvitelli", Naples 80121, Italy.
[6]Department of Experimental Medicine, Section of Pharmacology, University of Campania "L. Vanvitelli", Naples 80121, Italy.
[7]Department of Experimental Medicine, "La Sapienza" University, Rome 00161, Italy.
[8]Division of Translational Cancer Research, German Cancer Research Center (DKFZ) and German Cancer Consortium (DKTK), 69120 Heidelberg, Germany.
[9]Chair of Translational Cancer Research and Department of Medicine II, School of Medicine, Klinikum rechts der Isar, Technische Universität München, 81675 München, Germany.
*These authors contributed equally to this work.
§These authors jointly supervised this work.

Received 10 May; accepted 15 November 2017.

1. van Berlo, J. H. *et al.* c-kit$^+$ cells minimally contribute cardiomyocytes to the heart. *Nature* **509,** 337–341 (2014).
2. Sultana, N. *et al.* Resident c-kit$^+$ cells in the heart are not cardiac stem cells. *Nat. Commun.* **6,** 8701 (2015).
3. Liu, Q. *et al.* Genetic lineage tracing identifies *in situ* Kit-expressing cardiomyocytes. *Cell Res.* **26,** 119–130 (2016).
4. Ellison, G. M. *et al.* Adult c-kit^{pos} cardiac stem cells are necessary and sufficient for functional cardiac regeneration and repair. *Cell* **154,** 827–842 (2013).
5. Lennartsson, J. & Rönnstrand, L. Stem cell factor receptor/c-Kit: from basic science to clinical implications. *Physiol. Rev.* **92,** 1619–1649 (2012).
6. Klein, S. *et al.* Interstitial cells of Cajal integrate excitatory and inhibitory neurotransmission with intestinal slow-wave activity. *Nat. Commun.* **4,** 1630 (2013).
7. Heger, K. *et al.* CreER^{T2} expression from within the c-Kit gene locus allows efficient inducible gene targeting in and ablation of mast cells. *Eur. J. Immunol.* **44,** 296–306 (2014).
8. Hatzistergos, K. E. *et al.* cKit$^+$ cardiac progenitors of neural crest origin. *Proc. Natl Acad. Sci. USA* **112,** 13051–13056 (2015).
9. Jensen, P. & Dymecki, S. M. Essentials of recombinase-based genetic fate mapping in mice. *Methods Mol. Biol.* **1092,** 437–454 (2014).
10. Aquila, I. *et al.* The use and abuse of Cre/Lox recombination to identify adult cardiomyocyte renewal rate and origin. *Pharmacol. Res.* **127,** 116–128 (2018).
11. Nadal-Ginard, B., Ellison, G. M. & Torella, D. Absence of evidence is not evidence of absence: pitfalls of cre knock-ins in the c-Kit locus. *Circ. Res.* **115,** 415–418 (2014).
12. Smith, A. J. *et al.* Isolation and characterization of resident endogenous c-Kit$^+$ cardiac stem cells from the adult mouse and rat heart. *Nat. Protoc.* **9,** 1662–1681 (2014).

13. Vicinanza, C. *et al.* Adult cardiac stem cells are multipotent and robustly myogenic: c-kit expression is necessary but not sufficient for their identification. *Cell Death Differ.* **24,** 2101–2116 (2017).
14. Muzumdar, M. D., Tasic, B., Miyamichi, K., Li, L. & Luo, L. A global double-fluorescent Cre reporter mouse. *Genesis* **45,** 593–605 (2007).
15. Bernex, F. *et al.* Spatial and temporal patterns of c-kit-expressing cells in WlacZ/+ and WlacZ/WlacZ mouse embryos. *Development* **122,** 3023–3033 (1996).

Supplementary Information accompanies this Comment.

Author Contributions D.T. and B.N.-G. designed the research studies, analysed data and wrote the manuscript. C.V., I.A., E.C., M.S., F.M., T.M., F.F., E.D.G., E.I., P.M., V.A. and K.U. conducted the experiments, acquired and analysed data. F.C., A.T. and P.V. conducted RNA-sequencing experiments and analysed bioinformatic data. R.L., A.M.I., D.S. and C.I. contributed reagents. All authors approved the manuscript.

Competing Interests Declared none.

doi:10.1038/nature25771

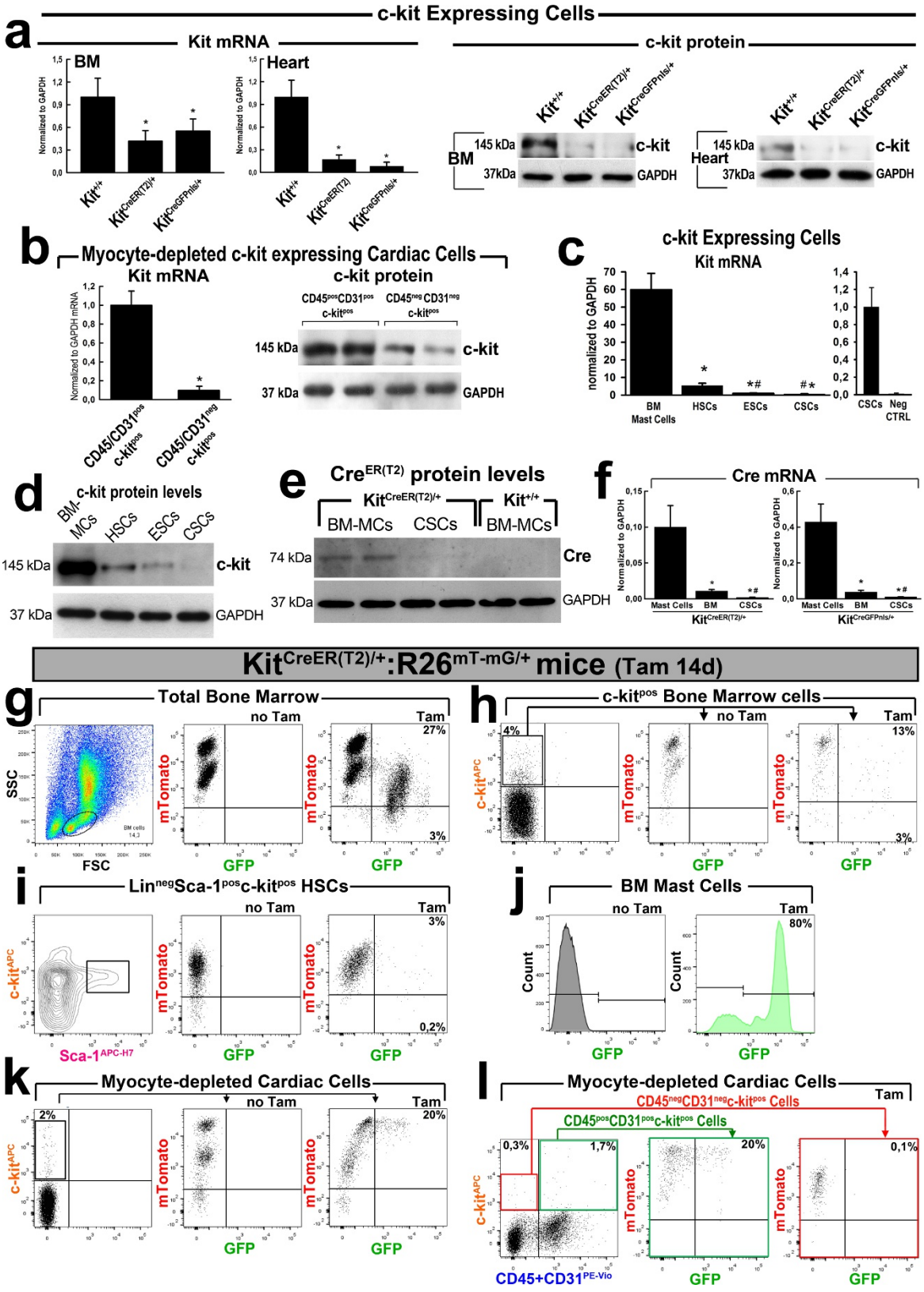

Extended Data Figure 1 | See next page for caption.

Extended Data Figure 1 | The *Kit*$^{CreER(T2)}$ allele reduces c-Kit expression and does not fate-map c-Kit-expressing CSCs with a short-term tamoxifen diet. a, *Kit* mRNA (left) and c-Kit protein (right) levels in all c-Kit-expressing cells isolated from bone marrow (BM) and heart of wild-type *Kit*$^{+/+}$, heterozygous *Kit*$^{CreER(T2)/+}$ and *Kit*$^{CreGFPnls/+}$ mice. Representative of $n = 5$ bone marrow samples and hearts. $^{*}P < 0.05$ versus wild-type *Kit*$^{+/+}$ mice. **b**, qPCR (left) cumulative data and representative western blot (right) analysis show that *Kit* mRNA and c-Kit protein levels in cardiomyocyte-depleted FACS-sorted CD45^{pos}CD31^{pos}c-Kit^{pos} cardiac cells versus CD45^{neg}CD31^{neg}c-Kit^{pos} cardiac cells. Representative of $n = 5$ hearts. $^{*}P < 0.05$ versus CD45^{pos}CD31^{pos}c-Kit^{pos} cardiac cells. **c**, **d**, *Kit* mRNA (**c**) and c-Kit protein (**d**) expression levels in different cell populations from wild-type mice. Representative of $n = 4$ biological replicates. $^{*}P < 0.05$ versus mast cells; $^{\#}P < 0.05$ versus HSCs in **c**. **c**, *Kit* transcript levels are verified over *Kit* mRNA absence in negative control (Neg CTRL), which are triple-negative-sorted CD45^{neg}CD31^{neg}c-Kit^{neg} cardiac cells. **e**, Western blot analysis showing Cre$^{ER(T2)}$ expression in bone marrow mast cells; Cre$^{ER(T2)}$ expression is only faintly detectable in freshly isolated CD45^{neg}CD31^{neg}c-Kit^{pos} CSCs from *Kit*$^{CreER(T2)/+}$ mice. Representative of $n = 3$ biological replicates. **f**, *cre* mRNA levels in bone marrow mast cells, bone marrow Lin^{neg} cells and CSCs from *Kit*$^{CreER(T2)/+}$ and *Kit*$^{CreGFPnls/+}$ mice. Representative of $n = 5$ mice. $^{*}P < 0.05$ versus mast cells; $^{\#}P < 0.05$ versus bone marrow. **g**–**l**, FACS analysis showing recombination efficiency in isolated bone marrow and cardiac cells from double-mutant *Kit*$^{CreER(T2)/+}$:*Rosa26*$^{mT/mG/+}$ mice treated with standard tamoxifen (Tam) diet (400 mg per kg diet) for 14 days. **g**, Fraction of Cre-recombined GFP-expressing cells in the monocyte–lymphocyte gate of total bone marrow cells after 14 days of tamoxifen diet. No recombination is evidence in the absence of tamoxifen. **h**, Fraction of Cre-recombined GFP-expressing cells in c-Kit^{pos} bone marrow cells after 14 days of tamoxifen diet. **i**, Gating of the Lin^{neg} bone marrow cells for the long-term repopulating Lin^{neg}Sca-1^{pos}c-Kit^{pos} (LSK) HSCs showing that only <5% HSCs showed recombination. **j**, The majority of bone marrow mast cells showed recombination and expressed GFP after 14 days of tamoxifen diet. **k**, The 14-day tamoxifen regime recombined ≤20% of the cardiomyocyte-depleted total c-Kit^{pos} cardiac cell population. **l**, All GFP-recombined c-Kit^{pos} cardiac cells were positive for CD45, CD31 (CD45^{pos}, CD31^{pos}) or both, representing cardiac mast cells or endothelial (progenitor) cells. Only a negligible fraction, <1%, of the c-Kit^{low} and CSC-enriched Lin^{neg} CD45^{neg}CD31^{neg}c-Kit^{pos} cardiac cells showed recombination and expression of GFP. **g**–**l**, Representative of $n = 5$ bone marrow samples and hearts. Data are mean ± s.d.

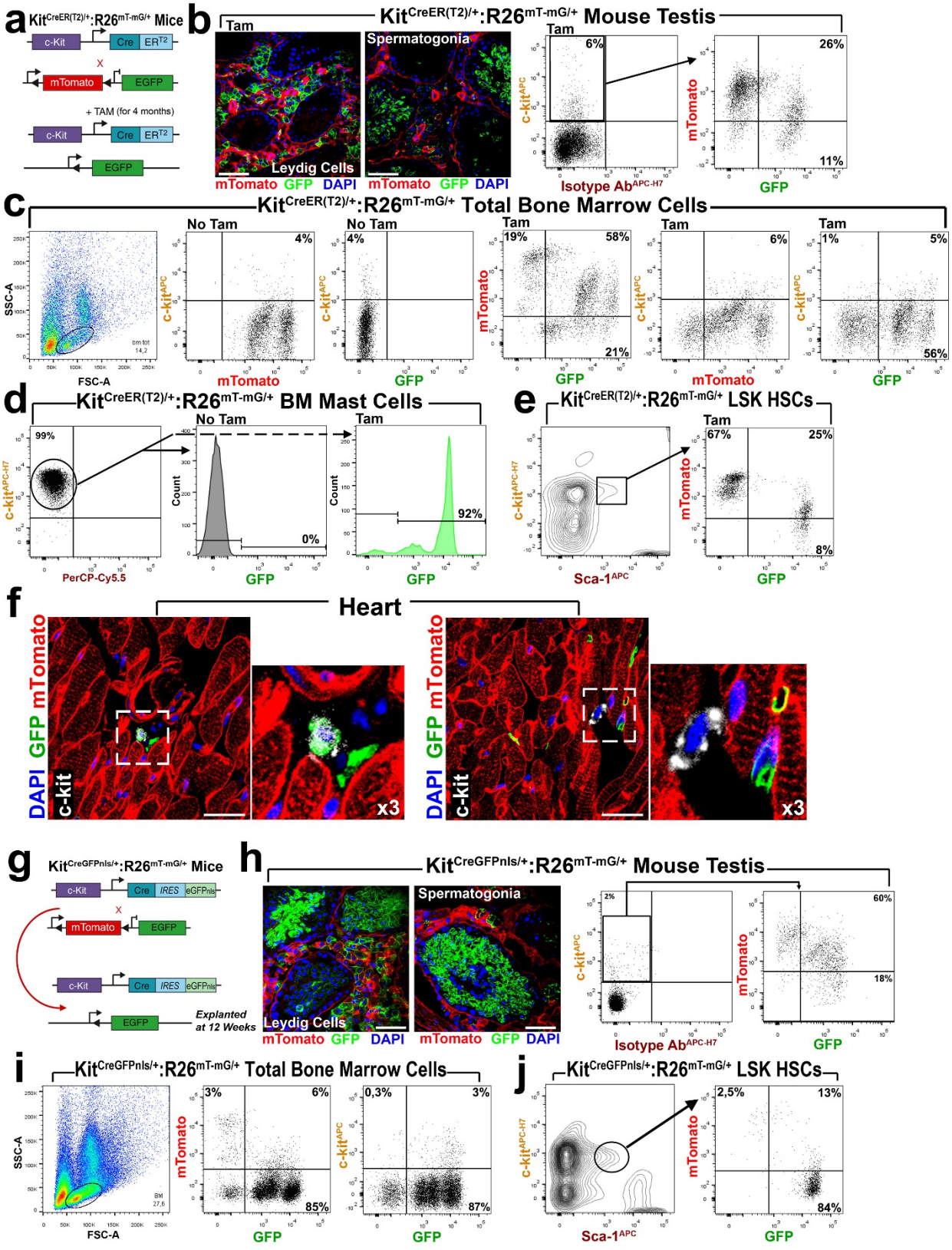

Extended Data Figure 2 | See next page for caption.

Extended Data Figure 2 | Fate-map tracking of c-Kit^{pos} cells using *Kit^{cre}* mice. a, Mice with KI in exon 1 of the *Kit* locus targeted to express tamoxifen-inducible Cre recombinase (CreER$^{(T2)}$) were crossed with Cre-reporter Rosa26 mice (*Rosa26$^{mT/mG}$*); the double-heterozygous mice were fed tamoxifen for four months. **b**, Confocal images (left) and FACS plots (right) show that *Kit$^{CreER(T2)}$* allele recombines in c-Kit-expressing Leydig cells and spermatogonia (and their derivatives within the seminiferous tubule) to express GFP in the testis whereas GFP expression was induced in around 40% of c-Kit^{pos} cells of this tissue. Representative of $n = 5$ mice. Scale bar, 50 μm. **c**, FACS plot of total bone marrow (with lymphocyte–monocyte gating strategy, left) of double-mutant *Kit$^{CreER(T2)/+}$:Rosa26$^{mT/mG/+}$* showing GFP expression in approximately 80% of cells, but no signal in the absence of tamoxifen. In particular, ≥70% of all c-Kit-antibody-detected cells were GFP^{pos}. Representative of $n = 5$ bone marrow samples. **d**, Most bone marrow mast cells (c-Kit expression, left) showed recombination and expressed GFP. **e**, Only a fraction (<35%) of the long-term LSK HSCs expressed GFP. **f**, Representative confocal images of cardiac cross-sections from *Kit$^{CreER(T2)/+}$:Rosa26$^{mT/mG/+}$* mice treated with tamoxifen diet for four months show that Cre-dependent recombination-induced GFP expression is detectable only in a fraction (around 60%) of non-cardiomyocyte c-Kit-labelled cardiac cells. Scale bars, 20 μm. Representative of $n = 5$ mice. **g**, Mice with *Kit* exon 1 locus KI to express Cre recombinase and GFP with a nuclear localization sequence (GFPnls) behind an internal ribosome entry site (IRES) were crossed to Cre reporter Rosa26 mice (*Rosa26$^{mT/mG}$*) for lineage tracing. **h**, Confocal images (left) and FACS plots (right) show that the *Kit^{CreGFPnls}* allele recombines in Leydig cells and spermatogonia in the testis to become GFP^{pos} whereas the overall recombination in the testis was approximately 80% of the c-Kit^{pos} cells. Scale bars, 50 μm. Note that the majority of recombined cells still express mT. Representative of $n = 5$ mice. **i**, FACS plot of total bone marrow cells from double-mutant *Kit$^{CreGFPnls/+}$:Rosa26$^{mT/mG/+}$* mice showing GFP expression in more than 90% of cells. Approximately 90% of total c-Kit-antibody-detected cells were GFP^{pos}. **j**, A majority of LSK HSCs expressed GFP. Representative of $n = 5$ bone marrow samples.

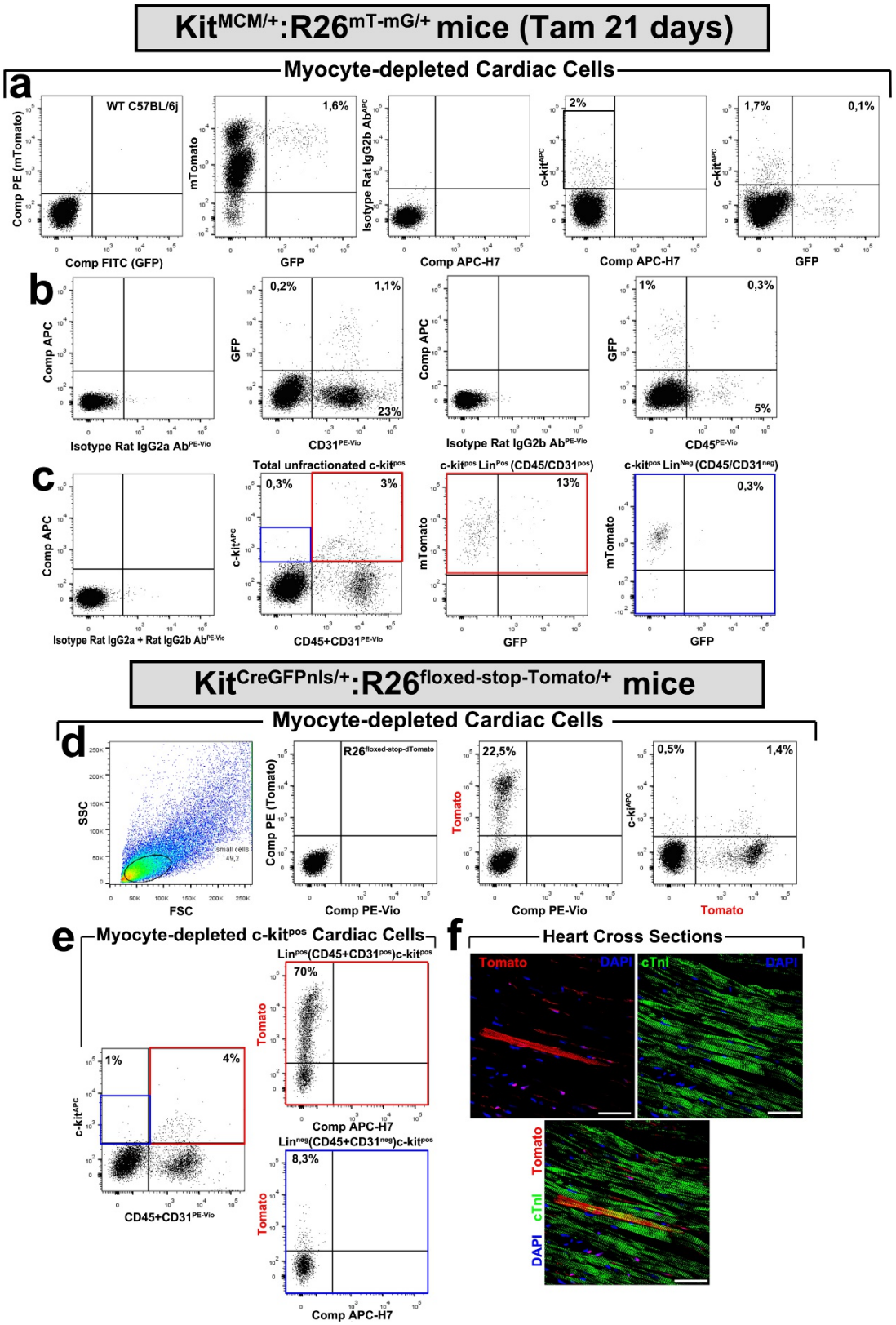

Extended Data Figure 3 | See next page for caption.

Extended Data Figure 3 | Fate-map tracking of c-Kit^{pos} CSCs using *Kit^{cre}* mice. FACS analysis showing recombination efficiency in isolated cardiomyocyte-depleted cardiac cells from double-mutant *Kit$^{MCM/+}$:Rosa26$^{mT/mG/+}$* mice treated with a standard tamoxifen diet (400 mg per kg diet) for 21 days ($n = 5$ mice). **a**, After 21 days of tamoxifen diet, less than 2% of total cardiac cells showed recombination and induction of GFP. Note that all the identified MCM-recombined GFP^{pos} cells were also still mT^{pos}. Approximately 10% of the cardiomyocyte-depleted c-Kit^{pos} cardiac cell population showed recombination and expressed GFP. **b**, Independently of the level of c-Kit expression, almost all recombined GFP^{pos} cells were CD31^{pos} (around 85%) and CD45^{pos} (about 25%). Thus, a standard tamoxifen regime with a widely used pulse period only genetically recombines lineage-committed cells (endothelial or immune cells) within the heart. **c**, All GFP-expressing recombined c-Kit^{pos} cardiac cells were CD45^{pos}, CD31^{pos} or both, representing cardiac mast cells or endothelial (progenitor) cells. Only a negligible fraction, <1%, of the c-Kit^{low} and CSC-enriched Lin^{neg}CD45^{neg}CD31^{neg}c-Kit^{pos} cardiac cells showed recombination and induction of GFP expression. **a**–**c**, Representative of $n = 4$ hearts. **d**–**f**, *Kit$^{CreGFPnls/+}$* mice were crossed with B6;129S6-Gt(ROSA)26Sortm9(CAG-tdTomato)Hze/J (abbreviated as *Rosa26$^{floxed\text{-}stop\text{-}tdTomato}$*) mice that have a targeted mutation in the Gt(ROSA)26Sor locus with a *loxP*-flanked STOP cassette preventing transcription of a CAG-promoter-driven red fluorescent protein variant (tdTomato), which is expressed following Cre-mediated recombination. **d**, Around 20% of total cardiac cells and about 70% of c-Kit^{pos} cardiac cells from these mice are tdTomato^{pos}. **e**, Around 70% of lineage-committed endothelial/mast cell (CD45^{pos}CD31^{pos}c-Kit^{pos}) cardiac cells showed recombination and expressed tdTomato, whereas less than 10% of the CSC-enriched CD45^{neg}CD31^{neg}c-Kit^{pos} showed recombination and were tdTomato^{pos}. **d**, **e**, Representative of $n = 5$ hearts. **f**, Confocal image showing recombined tdTomato^{pos} cardiomyocytes in the ventricular myocardium of 8–12-week-old *Kit$^{CreGFPnls/+}$:Rosa26$^{floxed\text{-}stop\text{-}tdTomato/+}$* mice. Representative of $n = 3$ hearts. Scale bar, 50 μm.

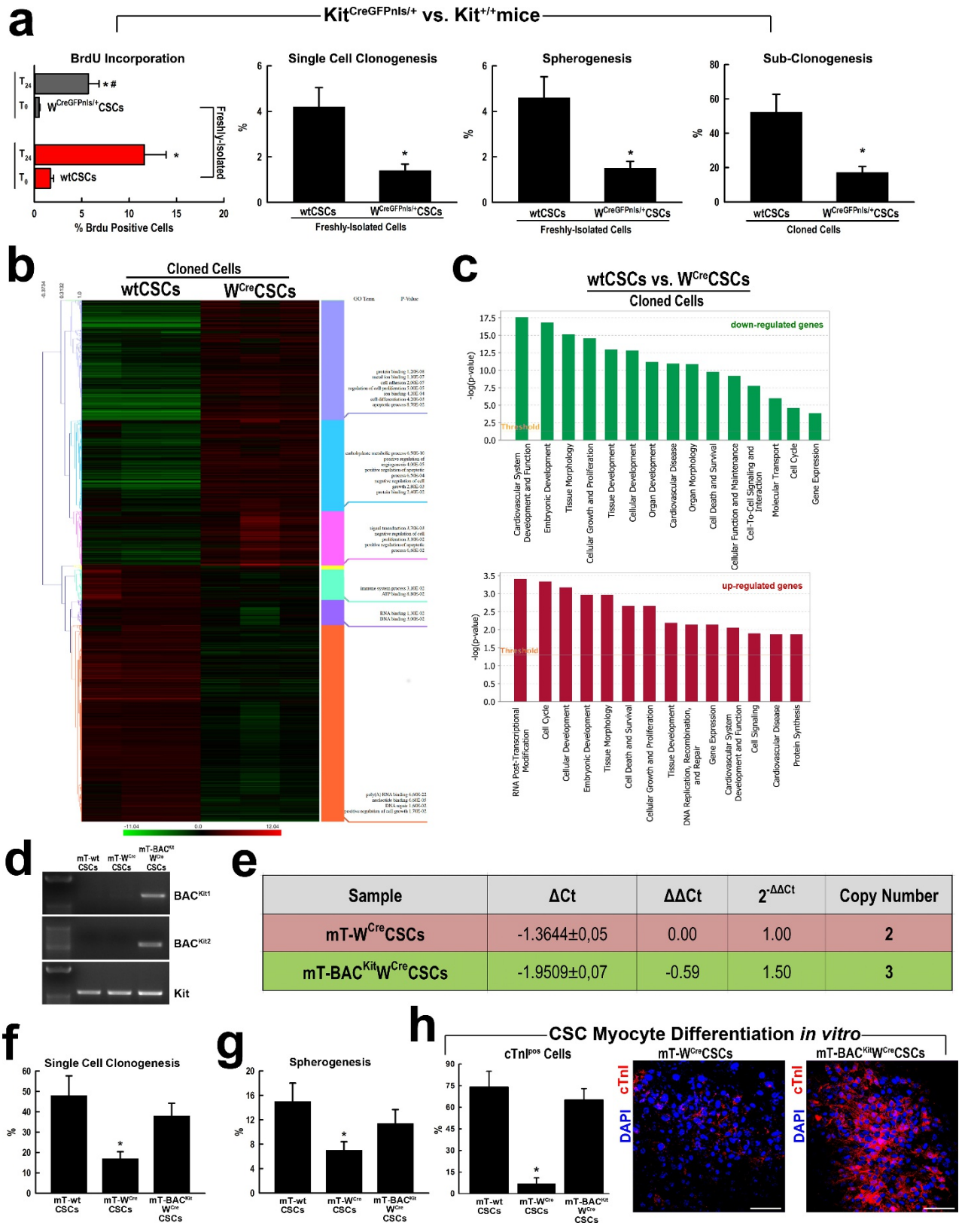

Sample	ΔCt	ΔΔCt	$2^{-\Delta\Delta Ct}$	Copy Number
mT-W^{Cre}CSCs	-1.3644±0,05	0.00	1.00	2
mT-BAC^{Kit}W^{Cre}CSCs	-1.9509±0,07	-0.59	1.50	3

Extended Data Figure 4 | See next page for caption.

Extended Data Figure 4 | W^{cre} allele KI and resulting *Kit* heterozygosity impair CSC biology and myogenic potential *in vitro*. **a**, Serum-induced 24 h BrdU incorporation by freshly isolated $W^{CreGFPnls/+}$ CSCs compared to wild-type CSCs. $^{*}P < 0.05$ versus T_0; $^{\#}P < 0.05$ versus wild-type CSCs. Clonal efficiency of freshly isolated $W^{CreGFPnls/+}$ CSCs compared to wild-type CSCs. $^{*}P < 0.05$ versus wild-type CSCs. $W^{CreGFPnls/+}$ CSCs formed fewer cardiospheres than wild-type CSCs. The number of cardiospheres is expressed as a percentage of 1×10^5 plated cells. $^{*}P < 0.05$ versus wild-type CSCs. Single-cell-cloned $W^{CreGFPnls/+}$ CSCs re-cloned at lower efficiency than wild-type CSCs. $^{*}P < 0.05$ versus wild-type CSCs. $n = 5$ experiments. **b**, Heat map of RNA-sequencing profile of the 2,425 downregulated and 2,870 upregulated genes for the comparison of W^{Cre} and wild-type CSCs and their gene ontology clustering for specific gene function. $n = 3$ of biological replicates. **c**, Functional categorization by ingenuity pathway analysis (IPA) of the downregulated and upregulated genes by RNA sequencing in the comparison between W^{Cre} CSC (from $Kit^{CreER(T2)/+}$ mice) and wild-type CSC clones. Histogram represents the most significant canonical pathways generated using IPA software. The ratio was calculated by dividing the number of genes from our dataset that map to each single pathway by the total number of genes included into the canonical pathway. **b**, **c**, Mean of $n = 3$ biological replicates. **d**, PCR analysis with two different pair of BAC primers showing BAC^{Kit} expression in mT-W^{Cre} CSCs. *Kit* gene primers were used as control. $n = 3$ biological replicates. **e**, qPCR data showing *Kit* DNA copy number in BAC-naive mT-W^{Cre} CSCs and mT-$BAC^{Kit}W^{Cre}$ CSCs. Representative of $n = 3$ biological replicates. **f**, Clonal efficiency of mT-$BAC^{Kit}W^{Cre}$ CSCs, mT-W^{Cre} CSCs and mT-WT CSCs. $^{*}P < 0.05$ versus all other treatments. $n = 5$ biological replicates. **g**, Cardiosphere formation of mT-$BAC^{Kit}W^{Cre}$ CSCs, mT-W^{Cre} CSCs and mT-WT CSCs. $^{*}P < 0.05$ versus all other treatments. $n = 5$ biological replicates. **h**, Bar graph and confocal images of cTnI expression in cardiospheres from cloned mT-WT CSCs, mT-W^{Cre} CSCs and mT-$BAC^{Kit}W^{Cre}$ CSCs after 14 days in myogenic medium. $^{*}P < 0.05$ versus all other treatments. Representative of $n = 5$ biological replicates. Scale bar, 50 μm. Data are mean ± s.d.

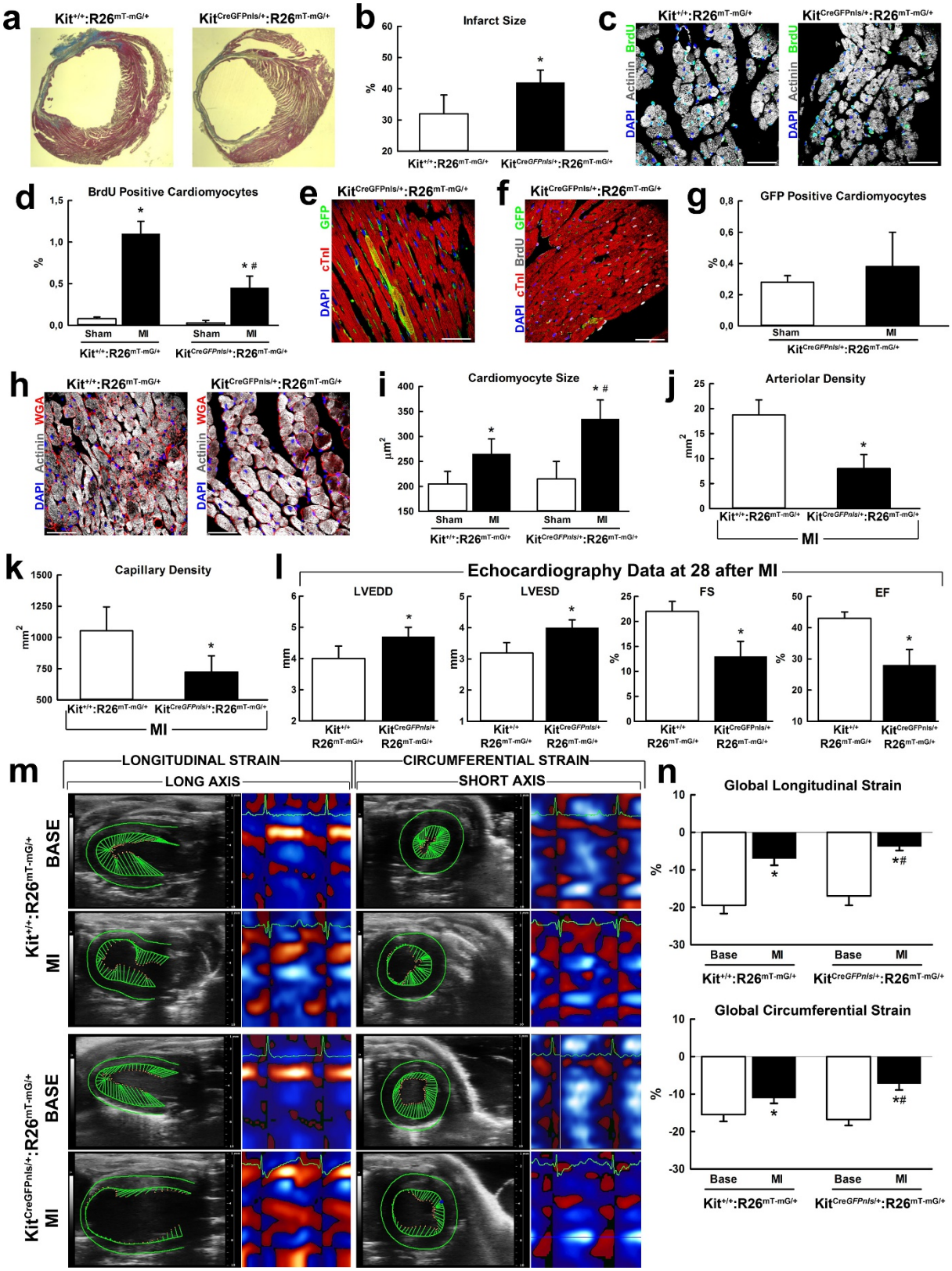

Extended Data Figure 5 | See next page for caption.

Extended Data Figure 5 | *Kit*^{cre}-KI hampers cardiac regeneration and repair after myocardial infarction. To test the effect of the *Kit*^{cre}-KI mutations on cardiac regeneration *in vivo*, 10-week-old female *Kit*$^{CreGFPnls/+}$:*Rosa26*$^{mT/mG/+}$ double-heterozygous mice and *Rosa26*$^{mT/mG/+}$ heterozygous controls were subjected to myocardial infarction (MI) by permanent ligation of the left coronary artery followed by systemic BrdU administration through mini-osmotic pumps. *Kit*$^{CreGFPnls/+}$-KI mice were used instead of tamoxifen-inducible *Kit*$^{CreER(T2)/+}$-KI mice, because of their highest *Kit*^{cre}-induced recombination and to avoid possible confounding effects related to tamoxifen (and tamoxifen-induced Cre) toxicity *in vivo*[9]. *Kit*$^{CreGFPnls/+}$:*Rosa26*$^{mT/mG/+}$ double-heterozygous females had to be used, because in our hands the acute mortality of myocardial infarction in sibling males was $\geq$75% whereas it was around 30% in the *Rosa26*$^{mT/mG/+}$ heterozygous controls. Additionally, around 50% of *Kit*$^{CreGFPnls/+}$:*Rosa26*$^{mT/mG/+}$ males and about 30% of *Kit*$^{CreGFPnls/+}$:*Rosa26*$^{mT/mG/+}$ females showed spontaneous alterations of cardiac function at baseline before myocardial infarction and had to be excluded. **a**, Light microscopy images showing Masson staining of infarcted hearts from c-Kit wild-type control *Kit*$^{+/+}$:*Rosa26*$^{mT/mG/+}$ and *Kit*$^{CreGFPnls/+}$:*Rosa26*$^{mT/mG/+}$ mice. Representative of $n = 6$ mice per group. **b**, Infarct size assessment 28 days after coronary ligation in *Kit*$^{+/+}$:*Rosa26*$^{mT/mG/+}$ and *Kit*$^{CreGFPnls/+}$:*Rosa26*$^{mT/mG/+}$ mice. $^{*}P < 0.05$ versus *Kit*$^{+/+}$:*Rosa26*$^{mT/mG/+}$ mice. $n = 6$ mice per group. **c**, Representative confocal microscopy images of BrdU incorporation in the border zone of infarcted hearts from *Kit*$^{+/+}$:*Rosa26*$^{mT/mG/+}$ and *Kit*$^{CreGFPnls/+}$:*Rosa26*$^{mT/mG/+}$ mice. Scale bar, 50 μm. **d**, Number of newly generated BrdU^{pos} cardiomyocytes in sham and infarcted (MI) *Kit*$^{+/+}$:*Rosa26*$^{mT/mG/+}$ and *Kit*$^{CreGFPnls/+}$:*Rosa26*$^{mT/mG/+}$ mice 28 days after sham or myocardial infarction surgery. $^{*}P < 0.05$ versus sham; $^{\#}P < 0.05$ versus *Kit*$^{+/+}$:*Rosa26*$^{mT/mG/+}$ mice. $n = 6$ mice per group. **e**, **f**, Representative confocal microscopy images of GFP^{pos} cardiomyocytes in the border zone of infarcted hearts from *Kit*$^{CreGFPnls/+}$:*Rosa26*$^{mT/mG/+}$ mice. Note that in **f** GFP^{pos} cardiomyocytes are BrdU^{neg}. Scale bar, 50 μm. **g**, Bar graph with cumulative data showing the number of GFP^{pos} cardiomyocytes in sham and infarcted *Kit*$^{CreGFPnls/+}$:*Rosa26*$^{mT/mG/+}$ mice 28 days after surgery. **h**, Representative confocal images of cardiac cross-sections showing higher cardiomyocyte hypertrophy in *Kit*$^{CreGFPnls/+}$:*Rosa26*$^{mT/mG/+}$ compared to *Kit*$^{+/+}$:*Rosa26*$^{mT/mG/+}$ mice 28 days after myocardial infarction. WGA, wheat-germ agglutinin. Scale bar, 50 μm. **i**, Cardiomyocyte size in *Kit*$^{+/+}$:*Rosa26*$^{mT/mG/+}$ and *Kit*$^{CreGFPnls/+}$:*Rosa26*$^{mT/mG/+}$ mice. $^{*}P < 0.05$ versus sham; $^{\#}P < 0.05$ versus *Kit*$^{+/+}$:*Rosa26*$^{mT/mG/+}$ mice. $n = 6$ mice per group. **j**, Arteriolar density in the infarct border zone of *Kit*$^{+/+}$:*Rosa26*$^{mT/mG/+}$ and *Kit*$^{CreGFPnls/+}$:*Rosa26*$^{mT/mG/+}$ mice 28 days after myocardial infarction. $^{*}P < 0.05$ versus *Kit*$^{+/+}$:*Rosa26*$^{mT/mG/+}$ mice. $n = 6$ mice per group. **k**, Capillary density in the infarct border zone of *Kit*$^{+/+}$:*Rosa26*$^{mT/mG/+}$ and *Kit*$^{CreGFPnls/+}$:*Rosa26*$^{mT/mG/+}$ mice 28 days after myocardial infarction. $^{*}P < 0.05$ versus *Kit*$^{+/+}$:*Rosa26*$^{mT/mG/+}$ mice. $n = 6$ mice per group. **l**, Echocardiography assessment of left ventricular function 28 days after myocardial infarction in *Kit*$^{+/+}$:*Rosa26*$^{mT/mG/+}$ and *Kit*$^{CreGFPnls/+}$:*Rosa26*$^{mT/mG/+}$ mice. $^{*}P < 0.05$ versus *Kit*$^{+/+}$:*Rosa26*$^{mT/mG/+}$ mice. $n = 6$ mice per group. LVEDD, left ventricle end diastolic diameter; LVESD, left ventricle end systolic diameter; EF, ejection fraction; FS, fractional shortening. **m**, Representative echo images and longitudinal and circumferential strain traces in long and short axis, from *Kit*$^{+/+}$:*Rosa26*$^{mT/mG/+}$ and *Kit*$^{CreGFPnls/+}$:*Rosa26*$^{mT/mG/+}$ mice at baseline (Base) and 28 days after myocardial infarction. **n**, Longitudinal and circumferential strain values in *Kit*$^{+/+}$:*Rosa26*$^{mT/mG/+}$ versus *Kit*$^{CreGFPnls/+}$:*Rosa26*$^{mT/mG/+}$ mice at baseline and 28 days after myocardial. $^{*}P < 0.05$ versus baseline; $^{\#}P < 0.05$ versus *Kit*$^{+/+}$:*Rosa26*$^{mT/mG/+}$ mice. $n = 6$ mice per group. Data are mean ± s.d.

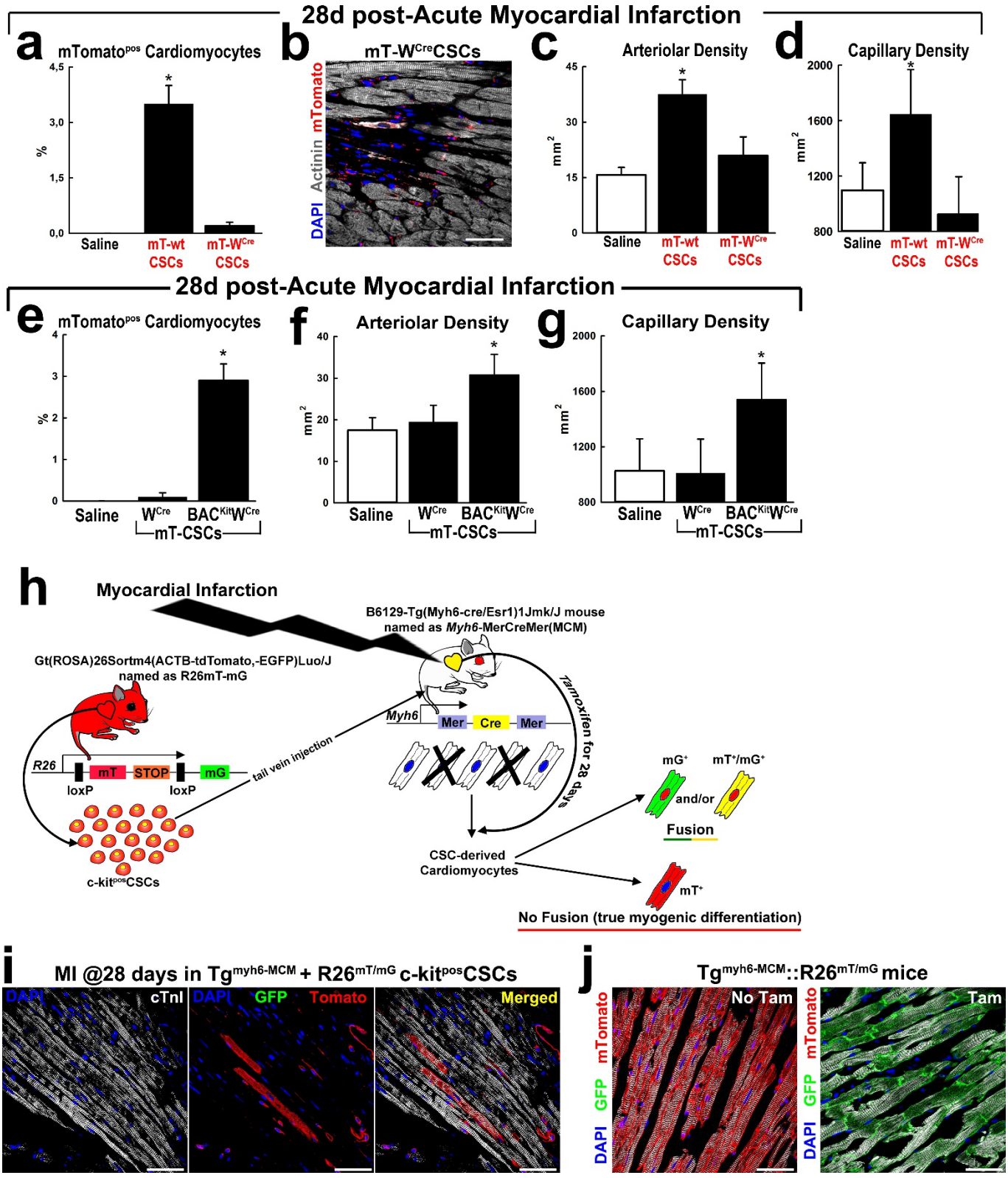

Extended Data Figure 6 | See next page for caption.

Extended Data Figure 6 | W^{cre}-null allele hampers CSC regenerative potential after myocardial infarction and neomyogenesis, which is independent from cell fusion. **a**, Cumulative data of CSC-derived mT^{pos} cardiomyocytes from female C57BL/6J wild-type mice 28 days after myocardial infarction treated with either saline ($n = 6$ mice) or with the indicated CSC types ($n = 6$ mice per group). $^*P < 0.05$ versus all other treatments. **b**, Representative confocal image of a CSC-derived newly formed mT^{pos} cardiomyocyte in mT-W^{cre} CSC-injected mice 28 days after myocardial infarction. Scale bar, 30 μm. **c**, Cumulative data of arteriolar density in the infarct border zone of saline-, mT-WT CSC- or mT-W^{Cre} CSC-treated female C57BL/6J wild-type mice 28 days after myocardial infarction. $^*P < 0.05$ versus all other treatments. **d**, Cumulative data of capillary density in the infarct border zone of saline-, mT-WT CSC- or mT-W^{Cre} CSC-treated female C57BL/6J wild-type mice 28 days after myocardial infarction. $^*P < 0.05$ versus all other treatments. **b**–**d**, Number of mice per group as indicated in **a**. **e**–**g**, Cumulative data of CSC-derived mT^{pos} cardiomyocytes (**e**), arteriolar density (**f**) and capillary density (**g**) in the infarct border zone of female wild-type C57BL/6J mice 28 days after myocardial infarction treated with saline ($n = 6$), mT-W^{Cre} CSCs ($n = 6$) or mT-$BAC^{Kit}W^{Cre}$ CSCs ($n = 6$). $^*P < 0.05$ versus all other treatments. **h**, Schematic of study design to assess CSC fusion with hosting cardiomyocytes. Transgenic (Tg) *Myh6-MerCreMer* ($Tg^{Myh6\text{-}MCM}$) female ($n = 3$) mice that carry a transgenic cardiomyocyte-restricted tamoxifen-inducible *cre* gene construct, had were subjected to myocardial infarction by coronary ligation. Right after coronary ligation, mice were treated by tail-vein injection with wild-type clonal mT^{pos} CSCs (mT-WT CSCs). Mice were fed with a tamoxifen diet for four weeks. The mT-WT CSCs were isolated from $Rosa26^{mT/mG}$ male mice and cloned. Therefore, these clonal cells and their progeny constitutively express membrane Tomato (mT^{pos}), which switches to express membrane GFP (becoming mG^{pos}) when recombined in response to Cre recombinase. The injection of mT-WT CSCs in $Tg^{Myh6\text{-}MCM}$ mice tests directly whether new cardiomyocytes are exclusively the progeny of the mT-WT CSCs injected, in which case these cells should be red (mT^{pos}), or the result of cell fusion of the injected cells with host cardiomyocytes, in which case the cells should be yellow (mT^{pos} and mG^{pos} together show as yellow) or only green (mG^{pos}). Indeed, if the putative new cardiomyocytes were not newly generated, but the product of the fusion of the injected cells with the host cardiomyocytes, these fused cells should be yellow or green. Tamoxifen activates Cre only in the host cardiomyocytes of $Tg^{Myh6\text{-}MCM}$ mice and the recombination induces the expression of mG only if the injected reporter-switchable CSCs fuse with the host cardiomyocytes. Thus, the recombined host cardiomyocytes will be either mT^{pos} and mG^{pos} (yellow) or mG^{pos} (green), the latter depending on the dilution time of mT expression after recombination. On the other hand, $mG^{neg}mT^{pos}$ cardiomyocytes can only be the direct progeny of the injected CSCs with no fusion to host cardiomyocytes. **i**, Representative confocal microscopy images of CSC-derived mT^{pos} cardiomyocytes in the border zone ($3.0 \pm 0.5\%$) of $Tg^{Myh6\text{-}MCM}$ mice with myocardial infarction treated with mT-WT CSCs and fed with a tamoxifen diet. It is evident that labelled cardiomyocytes in the infarct border zone were mT^{pos} but mG^{neg} as expected for the cardiomyocyte-differentiated progeny of the injected CSCs, which excludes cell fusion as a relevant mechanism for the appearance of these new muscle cells after myocardial infarction. Scale bar, 50 μm. Note, the level of baseline red or green autofluorescent cardiomyocytes in un-transplanted mice resulting from the staining protocols was <0.005%. None of these weak apparently positive signals had the typical membrane localization expected for the membrane-targeted dTomato and GFP Cre reporters. **j**, The mT and mG signal gains for the confocal images in **i** were set to appropriate positive controls using double transgenic $Tg^{Myh6\text{-}MCM}$::$Rosa26^{mT/mG}$ mice fed with a normal diet (no tamoxifen) or tamoxifen diet. Scale bar, 50 μm. Data are mean ± s.d.

van Berlo *et al.* reply

REPLYING TO: C. Vicinanza *et al. Nature* **555** https://doi.org/10.1038/nature25771 (2018)

The accompanying Comment by Vicinanza *et al.*[1] does not agree with our previous study[2] regarding the utility of c-Kit^{pos} (also known as Kit^{pos}) cells when investigating regeneration in the heart. The authors claim that three previous publications[2–4] using *Kit^{cre}* knock-in lineage-tracing question their previous work that shows that tissue-specific c-Kit^{pos} cardiac stem/progenitor cells (CSCs) are necessary and sufficient for cardiomyocyte regeneration and/or replenishment after injury[5]. However, the regenerative data within their previous manuscript did not address the role of endogenous c-Kit^{pos} cells in the heart[5]. Instead, they relied on clonally derived c-Kit^{pos} cells that were selected in culture and then injected into the circulatory system of mice and these cells remarkably homed to the heart and generated abundant new cardiomyocytes that repaired isoproterenol-mediated injury[5].

The authors now claim that the number of c-Kit^{pos} cells with cardiomyogenic-clone-producing potential is very low in the mouse heart (approximately 1% of total c-Kit^{pos} cells)[6]. Indeed, the authors showed that broadly isolated primary cardiac c-Kit^{pos} cells, that were not clonally selected, had almost no ability to generate new cardiomyocytes or repair the infarcted heart[6]. The authors' new interpretation[1] that only a very small portion of c-Kit^{low} cells can be made clonal with regenerative activity contradicts their published results from 2003 in which broadly isolated c-Kit^{pos} cells regenerated 70% of the myocardium after infarction injury[7], or published results from 2013 showing that the majority of endogenous c-Kit^{pos} cells express Nkx2.5 (a cardiomyocyte-determining transcription factor)[5].

The authors further claim that *Kit^{cre}* knock-in lineage tracing approaches[2–4] fail to track these rare c-Kit^{low} CSCs, because of poor recombination efficiency and heterozygosity in the *Kit* allele. While we have previously addressed this criticism and discussed data to the contrary[8], we have recently published additional data showing that the majority of c-Kit^{pos}CD45^{neg} cells isolated from the hearts of *Kit^{cre}* mice are correctly lineage-traced[9], suggesting that this technique for tracking cells in mice is effective[2–4]. Indeed, a working group of established cardiac scientists recently published a consensus statement confirming that endogenous cardiac c-Kit^{pos} cells are an unlikely source for meaningful heart regeneration[10]. This statement was also based on the known biology of the adult mammalian heart, which essentially lacks acute cardiomyocyte-forming regenerative capacity. However, it seems reasonable that one could select and isolate rare clonally derived c-Kit^{pos} progenitor cell lines with ectopic cardiomyogenic activity, as suggested in the Comment[1]. However, the Comment does not address the role of endogenous c-Kit^{pos} cells in the heart. The current negative results simply address whether clonally derived c-Kit-expressing cells can have cardiomyogenic capacity, which we believe lacks all *in vivo* relevance and in no way contests our previous observations.

Jop H. van Berlo[1], Onur Kanisicak[2], Marjorie Maillet[2], Ronald J. Vagnozzi[2], Jason Karch[2], Suh-Chin J. Lin[2], Ryan C. Middleton[3], Eduardo Marbán[3] & Jeffery D. Molkentin[2,4]

[1]Department of Medicine, Division of Cardiology, Lillehei Heart Institute, University of Minnesota, Minneapolis, Minnesota, USA.
[2]Department of Pediatrics, Cincinnati Children's Hospital Medical Center, Cincinnati, Ohio, USA.
email: Jeff.Molkentin@cchmc.org
[3]Cedars-Sinai Heart Institute, 8700 Beverly Boulevard, Los Angeles, California, USA.
[4]Howard Hughes Medical Institute, Cincinnati Children's Hospital Medical Center, Cincinnati, Ohio, USA.

1. Vicinanza, C. *et al. Kit^{cre}* knock-ins fail to fate-map cardiac stem cells. *Nature* **555,** https://doi.org/10.1038/nature25771 (2018).
2. van Berlo, J. H. *et al.* c-kit^{+} cells minimally contribute cardiomyocytes to the heart. *Nature* **509,** 337–341 (2014).
3. Sultana, N. *et al.* Resident c-kit^{+} cells in the heart are not cardiac stem cells. *Nat. Commun.* **6,** 8701 (2015).
4. Liu, Q. *et al.* Genetic lineage tracing identifies *in situ* Kit-expressing cardiomyocytes. *Cell Res.* **26,** 119–130 (2016).
5. Ellison, G. M. *et al.* Adult c-kit^{pos} cardiac stem cells are necessary and sufficient for functional cardiac regeneration and repair. *Cell* **154,** 827–842 (2013).
6. Vicinanza, C. *et al.* Adult cardiac stem cells are multipotent and robustly myogenic: c-kit expression is necessary but not sufficient for their identification. *Cell Death Differ.* **24,** 2101–2116 (2017).
7. Beltrami, A. P. *et al.* Adult cardiac stem cells are multipotent and support myocardial regeneration. *Cell* **114,** 763–776 (2003).
8. Molkentin, J. D. Letter by Molkentin regarding article, "The absence of evidence is not evidence of absence: the pitfalls of Cre knock-ins in the c-Kit locus". *Circ. Res.* **115,** e21–e23 (2014).
9. Kanisicak, O., Vagnozzi, R. J. & Molkentin, J. D. Identity crisis for regenerative cardiac cKit^{+} cells. *Circ. Res.* **121,** 1130–1132 (2017).
10. Eschenhagen, T. *et al.* Cardiomyocyte regeneration: a consensus statement. *Circulation* **136,** 680–686 (2017).

doi:10.1038/nature25772